

# Quintessential interpretation of the evolving dark energy in light of DESI

Yuichiro Tada\*

*Institute for Advanced Research, Nagoya University,  
Furo-cho Chikusa-ku, Nagoya 464-8601, Japan and  
Department of Physics, Nagoya University,  
Furo-cho Chikusa-ku, Nagoya 464-8602, Japan*

Takahiro Terada†

*Kobayashi-Maskawa Institute for the Origin of Particles and the Universe,  
Nagoya University,  
Furo-cho Chikusa-ku, Nagoya 464-8602, Japan  
(Dated: April 29, 2024)*

The recent result of Dark Energy Spectroscopic Instrument (DESI) in combination with other cosmological data shows evidence of the evolving dark energy parameterized by  $w_0w_a$ CDM model. We interpret this result in terms of a quintessential scalar field and demonstrate that it can explain the DESI result even though it becomes eventually phantom in the past. Relaxing the assumption on the functional form of the equation-of-state (EoS) parameter  $w = w(a)$ , we also discuss a more realistic quintessential model. The implications of the DESI result for Swampland conjectures, cosmic birefringence, and the fate of the Universe are discussed as well.

## I. INTRODUCTION

The cosmological constant ( $\Lambda$ ) [1], or more generally dark energy (DE), is the least understood fundamental parameter in the low-energy effective field theory based on General Relativity and the Standard Model of Particle Physics. For example, the stable de Sitter Universe sourced by  $\Lambda$  is questioned in the context of quantum gravity such as the Swampland program [2, 3] (see Refs. [4–6] for reviews). If it is indeed unstable and hence the dark energy is evolving, it can play a richer cosmological role. For example, an evolving ultra-light axion-like field is discussed as a solution [7] (see also Refs. [8–12]) to the recently observed cosmic birefringence [13–17]. Thus, the nature of dark energy can be related both to fundamental physics and to cosmological observations.

Following their early data release [18, 19], the Dark Energy Spectroscopic Instrument (DESI) collaboration has recently announced its first-year results of the analyses of the baryon acoustic oscillation (BAO) [20–22] based on their large-volume precise observations of galaxies, quasars, and Lyman- $\alpha$  forest. See Refs. [23–42] for earlier BAO results. Although the DESI data alone are consistent with  $\Lambda$ CDM model, if the model is generalized to  $w$ CDM and  $w_0w_a$ CDM models (see, e.g., Refs. [43, 44]), the central values of these parameters are deviated from the  $\Lambda$ CDM value [22]. Combined with cosmic microwave background (CMB) data [45–52] and supernova data, they even exclude the  $\Lambda$ CDM model against  $w_0w_a$ CDM model at  $2.5\sigma$ ,  $3.5\sigma$ , and  $3.9\sigma$  for Pantheon+ [53], Union3 [54], and DES-SN5YR [55], respectively, as the supernova data. The data show the preference to  $w_0 > -1$  and  $w_a < 0$ ,

where  $w(a) = w_0 + w_a(1 - a)$  is the equation-of-state (EoS) parameter of the dark energy with  $a$  being the scale factor of the Friedmann–Lemaître–Robertson–Walker cosmology.<sup>1</sup> If confirmed, this result potentially has substantial implications for the origin and future of ourselves and the Universe.

In this paper, we discuss interpretations of the DESI result in terms of a canonical real scalar field. The scalar field playing the role of dark energy is called quintessence (see, e.g., Ref. [59] for a review). We first phenomenologically translate the observed relation  $w = w_0 + w_a(1 - a)$  into the scalar-field language. We discuss the implications for the Swampland conjectures (see Refs. [60, 61] for earlier works) and the cosmic birefringence. To overcome the limited validity range of the resulting model, we relax the assumption on the relation  $w = w(a)$  and consider a canonical model without the quintessence becoming phantom ( $w < -1$ ). We also extrapolate the DESI results into the future and discuss the fate of the Universe.

## II. RECONSTRUCTION OF THE SCALAR POTENTIAL

We consider the flat  $w_0w_a$ CDM model, where the EoS parameter of the dark energy is parameterized by the

\* tada.yuichiro.y8@f.mail.nagoya-u.ac.jp

† takahiro.terada.hepc@gmail.com

<sup>1</sup> The increase of  $w_0$  is correlated with the decrease of  $H_0$  [56, 57], which is the opposite direction to solve the Hubble tension. We thank Eoin Ó Colgáin for pointing out this fact. (For other issues in the interpretation of the DESI data in  $\Lambda$ CDM model, see Ref. [58], which appeared soon after the first version of our paper.) Nevertheless, the significance of the Hubble tension in  $w_0w_a$ CDM model is reduced compared to the  $\Lambda$ CDM model as the uncertainty gets larger with the additional parameters [22].

Chevallier–Polarski–Linder form [43, 62]

$$w(a) = w_0 + w_a(1 - a). \quad (1)$$

The scale factor  $a$  is normalized to unity at the present time, so the present value of the dark-energy EoS parameter is given by  $w_0$ . On the other hand,  $w_a$  parameterizes the time dependence of  $w$ .

The above linear relation (1) should be viewed as a toy model, or the simplest nontrivial parameterization of  $w(a)$  with time dependence [63–65]. The DESI data prefer  $w_a < 0$ . Obviously,  $w$  can become smaller than  $-1$  at an early time and violate the null energy condition.<sup>2</sup> A (homogeneous) canonical scalar field  $\phi$  with positive potential  $V(\phi) \geq 0$  can realize only  $-1 \leq w \leq 1$ , so the interpretation in terms of  $\phi$  must break down at some point. On the other hand,  $w$  also exits this range in the future extrapolation. This ( $w > 1$ ) is associated with a less exotic realization by a negative potential  $V(\phi) < 0$  in the relevant field domain. We will come back to these points below.

Assuming that the dark energy does not exchange the energy densities with other cosmic components, we have the continuity equation

$$\dot{\rho}_{\text{DE}} + 3(1 + w)H\rho_{\text{DE}} = 0, \quad (2)$$

where  $\rho_{\text{DE}}$  is the dark energy density and  $H = \dot{a}/a$  is the Hubble parameter. The solution under the linear assumption (1) is given by

$$\rho_{\text{DE}}(t) = \rho_{\text{DE},0} a(t)^{-3(1+w_0+w_a)} e^{3w_a(a(t)-1)}, \quad (3)$$

where  $\rho_{\text{DE},0}$  is the present value of  $\rho_{\text{DE}}$ . Since we are interested in the relatively late-time Universe, we can safely neglect the radiation component. Using the redshift scaling of the nonrelativistic matter component  $\rho_{\text{m}} \propto a^{-3}$  and the Friedmann equations, we can solve  $a = a(t)$ .

Let us translate the dynamics of dark energy into the quintessential field  $\phi = \phi(t)$ . Its EoS parameter is given by  $w = \frac{\frac{1}{2}\dot{\phi}^2 - V}{\frac{1}{2}\dot{\phi}^2 + V}$ . Using the Friedmann equations, the kinetic energy, the scalar potential, and its derivative are given in terms of  $w(a(t))$ , and  $a(t)$  as follows:

$$\begin{aligned} \frac{1}{2}\dot{\phi}^2 &= \frac{1}{2}(1 + w)\rho_{\text{DE}}, & V &= \frac{1}{2}(1 - w)\rho_{\text{DE}}, \\ V' &= \frac{1}{2}(w_a a - 3(1 - w^2))H\sqrt{\frac{\rho_{\text{DE}}}{1 + w}}. \end{aligned} \quad (4)$$

This can be used to map the contour on the  $(w_0, w_a)$ -plane to the contour on the  $(V, V')$ -plane. Fig. 1 shows the contour evaluated at the present time.

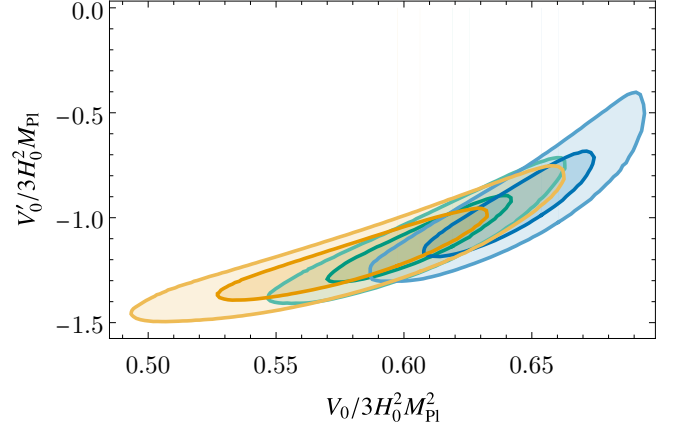


FIG. 1. The  $1\sigma$  and  $2\sigma$  contours of the allowed values of  $V$  and  $V'$  at the present time. The blue, green, and orange contours correspond to Panthéon+, DES, and Union, respectively, combined with CMB and DESI.

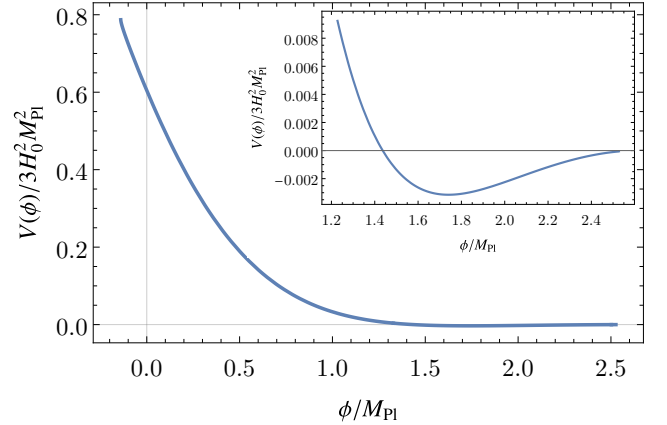


FIG. 2. The reconstructed scalar potential  $V(\phi)$  at the benchmark point. The potential is negative for  $\phi/M_{\text{Pl}} > 1.44$ .

For an intuitive understanding, we show the reconstructed scalar potential  $V(\phi)$  in Fig. 2 and the time evolution of  $\phi(t)$  as well as  $a(t)$  in Fig. 3 with the central value of DESI+CMB+DES ( $w_0 = -0.727$  and  $w_a = -1.05$ ) as the benchmark parameter. For this purpose, we define the origin of  $\phi$  to coincide with the current value, i.e.,  $\phi(t_0) = 0$  and assume  $\dot{\phi}(t_0) > 0$  without loss of generality.

We can reconstruct  $\phi(t)$  and  $V(\phi(t))$  only up to the point where  $\phi$  becomes a phantom in the past. At the benchmark point, this occurs at  $a = 0.74$  or  $z = 0.35$ . This redshift is greater than the pivot redshift values  $z_p$ , i.e., the redshift values most sensitive to the determination of  $w$ , reported in Ref. [22]. This suggests that the interpretation in terms of quintessence makes sense although it eventually becomes phantom in the past. We interpret the phantom crossing as an indication of the breakdown of the effective theory, and it should be replaced by another

<sup>2</sup> It was suggested that such a *phantom* phase is a mere consequence of an inappropriate choice of priors [66], after the appearance of the first version of our paper.

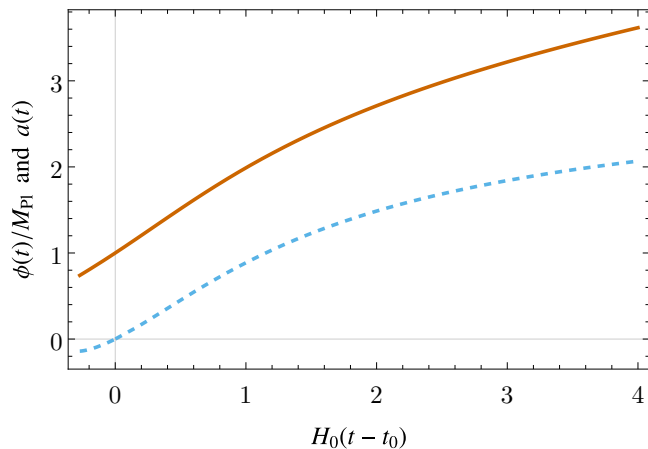


FIG. 3. Dynamics of  $a(t)$  (vermillion solid line) and  $\phi(t)$  (sky-blue dashed line) at the benchmark point.

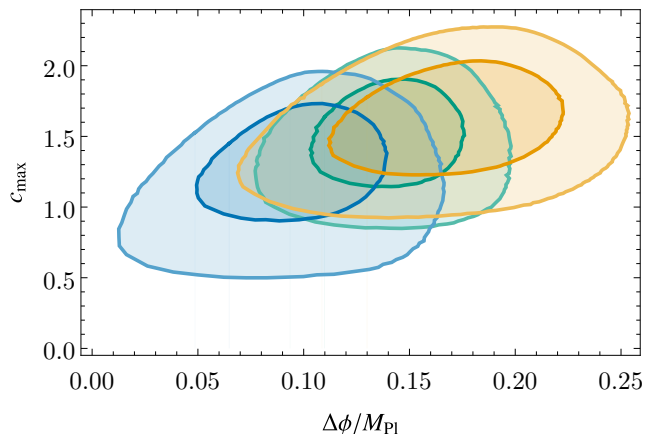


FIG. 4. The  $1\sigma$  and  $2\sigma$  contours of the allowed values of  $\Delta\phi$  and  $c_{\max}$ . The color coding is same as in Fig. 1.

theory in the early Universe.

It is also intriguing to discuss the implications for the future of the Universe. Fig. 3 shows that the accelerated expansion [67, 68] will soon stop and it will turn to the decelerated expansion again. By construction with the linearly increasing  $w$ ,  $V$  asymptotes to 0 from below with slowly rolling-up  $\phi$ . Of course, we can easily imagine that the linear behavior  $w(a)$  changes at some point in the future, and the shape of the potential may be modified. If there is a minimum with  $V > 0$ , there will be another accelerated expansion phase in the future with the reduced dark energy. On the other hand, if the field is trapped in a minimum with  $V < 0$  or if the potential is unbounded below, the Universe will eventually turn around into a contracting phase [69, 70]. In such a case, the kinetic energy of  $\phi$  typically dominates the energy density of the Universe and it will lead to a big crunch.

The thawing quintessence, or the decaying dark energy, may be a consequence of the quantum gravitational cen-

sorship against the stable de Sitter-like Universe. The (refined) de Sitter conjecture reads [71–73] (see also Refs. [74–77])

$$|V'| \geq cV, \quad \text{or} \quad V'' \leq -c'V, \quad (5)$$

in the reduced Planck unit  $M_{\text{Pl}} = 1$ , where  $c$  and  $c'$  are some positive constants. Naively, these dimensionless constants are expected to be of  $\mathcal{O}(1)$  leading to some tension with slow-roll inflationary models [72, 78–84]. In the negative part of the potential, the left inequality is automatically satisfied. For positive potential, the conjecture requires a sufficiently large slope (first inequality) or otherwise it should be unstable (second inequality). Fig. 2 shows that the positive part of the potential has a positive second derivative, so we focus on the first inequality. By studying  $c_{\max} \equiv \min_{V>0} |V'|/V$ , we can place an upper bound on  $c$ , i.e.,  $c \leq c_{\max}$ , for the reconstructed potential to be consistent with the conjecture. The constraint is shown in Fig. 4 in combination with the field excursion  $\Delta\phi$  to be discussed next.

An important implication of the light scalar field [7] is the recently detected cosmic birefringence [13–17], which requires new physics beyond the Standard Model [85]. The idea is that the following axion-like coupling biases the propagation of photon depending on its chirality in the presence of nonvanishing  $\phi$ , generating birefringence:

$$\mathcal{L} = \frac{1}{4} \sqrt{-g} g_{\phi\gamma\gamma} \phi F_{\mu\nu} \tilde{F}^{\mu\nu}, \quad (6)$$

where  $g_{\phi\gamma\gamma}$  is the  $\phi$ -photon-photon coupling constant,  $F_{\mu\nu}$  is the field-strength tensor of photon, and  $\tilde{F}^{\mu\nu}$  its dual. The observed isotropic cosmic birefringence angle  $\beta$  is  $\beta = 0.34^\circ \pm 0.09^\circ$  [16]. This is related to the field excursion  $\Delta\phi$  from the last scattering surface to the present time as  $\beta = g_{\phi\gamma\gamma} \Delta\phi/2$  [7]. In our case, we cannot extend  $\phi(t)$  beyond the phantom crossing, and we substitute the field excursion from the phantom point to the present time to  $\Delta\phi$ . One may interpret our  $\Delta\phi$  as a lower bound on the true  $\Delta\phi$  once the theory is completed into the would-be phantom regime. The result of our analysis on  $\Delta\phi$  is shown in Fig. 4 in combination with  $c_{\max}$ . The preferred range of the coupling is

$$g_{\phi\gamma\gamma} = 0.12 \left( \frac{0.1 M_{\text{Pl}}}{\Delta\phi} \right) M_{\text{Pl}}^{-1}. \quad (7)$$

With such a suppressed interaction with photons, it is free from observational constraints [7].

The required field excursion is sub-Planckian whereas it can become Planckian in the future (see Fig. 2). The  $\mathcal{O}(1)$  Planckian field excursion can potentially be in tension with (the refined version [86, 87] of) the Swampland distance conjecture [3], which states that an infinite tower of particles become light as  $m \sim \exp(-d\Delta\phi)$  with an  $\mathcal{O}(1)$  parameter  $d$  as any scalar field  $\phi$  moves over a distance  $\Delta\phi$ . If the field space of  $\phi$  is compact like an axion, the constraint disappears. Even if it is not compact, the actual breakdown of the effective field theory occurs only

after  $\phi$  moves over super-Planckian distance leading to the following constraint [88]

$$\Delta\phi \lesssim \frac{3}{d} M_{\text{Pl}} \log \left( \frac{M_{\text{Pl}}}{H_0} \right). \quad (8)$$

Because of the large logarithmic factor, this constraint is easily satisfied.

### III. A CONCRETE CANONICAL MODEL

Relaxing the linear assumption (1), we here investigate a more realistic realization of the time-varying EoS pa-

rameter from the viewpoint of the thawing quintessence model. In the thawing model, the quintessential scalar field  $\phi$  is first frozen on the potential due to the Hubble friction in the early universe. As the dark matter energy density gets diluted, the scalar field “thaws” and starts to roll down to the potential minimum. Expanding the potential up to the second order around the initial field value  $\phi_i$  as  $V(\phi) \simeq \sum_{n=0}^2 V^{(n)}(\phi_i)(\phi - \phi_i)^n/n!$  and supposing that the evolution of the scale factor is not significantly altered from that of the  $\Lambda$ CDM, one finds the evolution of the EoS parameter  $w$  in this model as [64, 65]

$$w(a) \simeq -1 + (1 + w_0) a^{3(K-1)} \mathcal{F}(a), \quad (9)$$

with

$$\mathcal{F}(a) = \left[ \frac{(K - F(a))(F(a) + 1)^K + (K + F(a))(F(a) - 1)^K}{(K - \Omega_\phi^{-1/2})(\Omega_\phi^{-1/2} + 1)^K + (K + \Omega_\phi^{-1/2})(\Omega_\phi^{-1/2} - 1)^K} \right]^2, \quad (10)$$

where

$$K = \sqrt{1 - \frac{4}{3} \frac{M_{\text{Pl}}^2 V''(\phi_i)}{V(\phi_i)}}, \quad F(a) = \sqrt{1 + (\Omega_\phi^{-1} - 1) a^{-3}}. \quad (11)$$

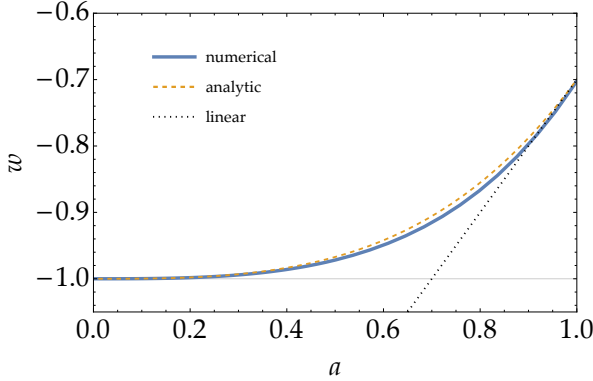


FIG. 5. Time evolution of the EoS parameter in the axion-like thawing model (12) with the parameters  $(\Lambda^2/H_0^2, f/M_{\text{Pl}}, \phi_i/f) = (8.7, 0.41, 0.55)$ . The blue line is the numerical result of the background equations of motion, the orange dashed one corresponds to the analytic formula (9), and the black dotted one is the linear fitting today (1) with  $(w_0, w_a) = (-0.7, -1)$ .

Here,  $\Omega_\phi$  is the current density parameter of  $\phi$  and we will assume the flat universe, i.e.,  $\Omega_\phi + \Omega_m = 1$ . The  $w_a$  parameter in the linear model (1) can be viewed as  $-w'(a)$  in this formula.

As we are now interested in a relatively large value of  $|w_a|$  going beyond the so-called slow-roll approximation,

we still need a parameter fine-tuning via a numerical parameter search to get a desired value of  $w$  and consistently recover the current density parameter  $\Omega_\phi$ . Let us suppose the axion-like potential,

$$V(\phi) = \Lambda^2 f^2 \left( 1 + \cos \frac{\phi}{f} \right), \quad (12)$$

with model parameters  $\Lambda$  and  $f$  as a representative thawing model. We find that the central value  $(w_0, w_a) \simeq (-0.7, -1)$  with  $\Omega_m \simeq 0.3$  can be realized by the parameter set  $(\Lambda^2/H_0^2, f/M_{\text{Pl}}, \phi_i/f) = (8.7, 0.41, 0.55)$ . The corresponding evolution of  $w$  is shown in Fig. 5. The field excursion is calculated as  $\Delta\phi \simeq 0.33 M_{\text{Pl}}$  while it reads  $\simeq 0.17 M_{\text{Pl}}$  in the linear model discussed in the previous section. The discrepancy may come from the smooth deviation of  $w$  from the linear relation. Nevertheless, this factor difference can be absorbed into the parametrization of the coupling constant to explain the cosmic birefringence.

The Swampland coefficients  $M_{\text{Pl}}|V'|/V$  and  $M_{\text{Pl}}^2 V''/V$  in this model are shown in Fig. 6. One sees that either of them always exceeds the unity and hence the model is compatible with the Swampland de Sitter conjecture.

The axion decay constant is constrained to be sub-Planckian by the weak gravity conjecture [89]. Applied to an axion, it can be written in the following form

$$f \lesssim \frac{M_{\text{Pl}}}{S_{\text{inst}}}, \quad (13)$$

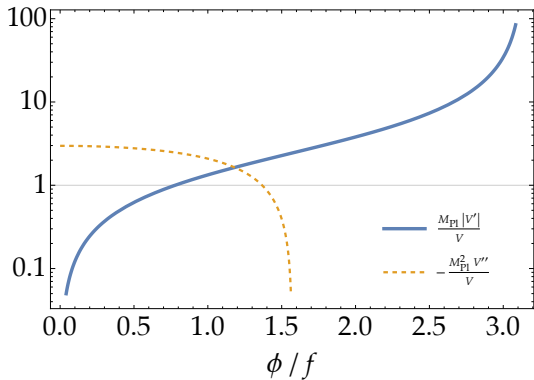


FIG. 6. The Swampland coefficients  $M_{\text{Pl}}|V'|/V$  (blue) and  $M_{\text{Pl}}^2 V''/V$  (orange-dashed) in the model (12) with the same parameters as Fig. 5. Either of them always exceeds the unity (thin horizontal line), exhibiting the compatibility with the Swampland de Sitter conjecture.

where  $S_{\text{inst}}$  is the instanton action. This means that the axion decay constant  $f$  is sub-Planckian as long as the contributions from higher instanton numbers are well suppressed. Our benchmark value  $f/M_{\text{Pl}} = 0.41$  is consistent with this conjecture.

## IV. DISCUSSIONS

We investigate the interpretation of the recent DESI result on the time-varying dark energy as a quintessential scalar field. Supposing the linear evolution of the EoS parameter  $w$  (1), the corresponding scalar potential is reconstructed in Sec. II up to the time when the simple linear relation indicates the phantom EoS,  $w < -1$ . The more realistic thawing model with the axion-like potential (12) is discussed in Sec. III.

Not only are the observational data understood in terms of a scalar field, but the time-varying dark energy also has several implications in the cosmological and particle physics context. For example, the decaying dark energy is preferred by the de Sitter Swampland conjecture [71, 73] as exhibited in Figs. 4 and 6. The sufficient field excursion can also explain the observed cosmic birefringence through CMB [7, 13]. The fate of the Universe strongly depends on the future shape of the potential, even the big crunch being possible.

One finds that the deviation of the linear relation in the thawing model is not negligible in Fig. 5. It even appears around the pivot scale  $z_p \simeq 0.26$  or  $a_p \simeq 0.79$  of DESI+CMB+DES (corresponding to the central value  $(w_0, w_a) = (0.727, -1.05)$ ) where  $w$  is best constrained by the observational data. The model here is hence expected to be confirmed or falsified in the near future by observing the time evolution of the dark energy beyond the linear assumption.

## ACKNOWLEDGMENTS

We are grateful to Takeshi Chiba, Tomohiro Fujita, and Shuichiro Yokoyama for helpful discussions. Y.T. is supported by JSPS KAKENHI Grant No. JP24K07047.

- 
- [1] S. Weinberg, The Cosmological Constant Problem, *Rev. Mod. Phys.* **61**, 1 (1989).
  - [2] C. Vafa, The String landscape and the swampland, [arXiv:hep-th/0509212](#) (2005).
  - [3] H. Ooguri and C. Vafa, On the Geometry of the String Landscape and the Swampland, *Nucl. Phys. B* **766**, 21 (2007), [arXiv:hep-th/0605264](#).
  - [4] E. Palti, The Swampland: Introduction and Review, *Fortsch. Phys.* **67**, 1900037 (2019), [arXiv:1903.06239 \[hep-th\]](#).
  - [5] M. van Beest, J. Calderón-Infante, D. Mirfendereski, and I. Valenzuela, Lectures on the Swampland Program in String Compactifications, *Phys. Rept.* **989**, 1 (2022), [arXiv:2102.01111 \[hep-th\]](#).
  - [6] N. B. Agmon, A. Bedroya, M. J. Kang, and C. Vafa, Lectures on the string landscape and the Swampland, [arXiv:2212.06187 \[hep-th\]](#) (2022).
  - [7] T. Fujita, K. Murai, H. Nakatsuka, and S. Tsujikawa, Detection of isotropic cosmic birefringence and its implications for axionlike particles including dark energy, *Phys. Rev. D* **103**, 043509 (2021), [arXiv:2011.11894 \[astro-ph.CO\]](#).
  - [8] K. V. Berghaus, P. W. Graham, D. E. Kaplan, G. D. Moore, and S. Rajendran, Dark energy radiation, *Phys. Rev. D* **104**, 083520 (2021), [arXiv:2012.10549 \[hep-ph\]](#).
  - [9] L. W. H. Fung, L. Li, T. Liu, H. N. Luu, Y.-C. Qiu, and S. H. H. Tye, Axi-Higgs cosmology, *JCAP* **08**, 057, [arXiv:2102.11257 \[hep-ph\]](#).
  - [10] S. Nakagawa, F. Takahashi, and M. Yamada, Cosmic Birefringence Triggered by Dark Matter Domination, *Phys. Rev. Lett.* **127**, 181103 (2021), [arXiv:2103.08153 \[hep-ph\]](#).
  - [11] M. Jain, A. J. Long, and M. A. Amin, CMB birefringence from ultralight-axion string networks, *JCAP* **05**, 055, [arXiv:2103.10962 \[astro-ph.CO\]](#).
  - [12] G. Choi, W. Lin, L. Visinelli, and T. T. Yanagida, Cosmic birefringence and electroweak axion dark energy, *Phys. Rev. D* **104**, L101302 (2021), [arXiv:2106.12602 \[hep-ph\]](#).
  - [13] Y. Minami and E. Komatsu, New Extraction of the Cosmic Birefringence from the Planck 2018 Polarization Data, *Phys. Rev. Lett.* **125**, 221301 (2020), [arXiv:2011.11254 \[astro-ph.CO\]](#).
  - [14] P. Diego-Palazuelos *et al.*, Cosmic Birefringence from the Planck Data Release 4, *Phys. Rev. Lett.* **128**, 091302 (2022), [arXiv:2201.07682 \[astro-ph.CO\]](#).



- [15] J. R. Eskilt, Frequency-dependent constraints on cosmic birefringence from the LFI and HFI Planck Data Release 4, *Astron. Astrophys.* **662**, A10 (2022), [arXiv:2201.13347 \[astro-ph.CO\]](#).
- [16] J. R. Eskilt and E. Komatsu, Improved constraints on cosmic birefringence from the WMAP and Planck cosmic microwave background polarization data, *Phys. Rev. D* **106**, 063503 (2022), [arXiv:2205.13962 \[astro-ph.CO\]](#).
- [17] J. R. Eskilt *et al.* (Cosmoglobe), COSMOGLOBE DR1 results - II. Constraints on isotropic cosmic birefringence from reprocessed WMAP and Planck LFI data, *Astron. Astrophys.* **679**, A144 (2023), [arXiv:2305.02268 \[astro-ph.CO\]](#).
- [18] J. Moon *et al.* (DESI), First detection of the BAO signal from early DESI data, *Mon. Not. Roy. Astron. Soc.* **525**, 5406 (2023), [arXiv:2304.08427 \[astro-ph.CO\]](#).
- [19] G. Adame *et al.* (DESI), The Early Data Release of the Dark Energy Spectroscopic Instrument, [arXiv:2306.06308 \[astro-ph.CO\]](#) (2023).
- [20] A. G. Adame *et al.* (DESI), DESI 2024 III: Baryon Acoustic Oscillations from Galaxies and Quasars, [arXiv:2404.03000 \[astro-ph.CO\]](#) (2024).
- [21] A. G. Adame *et al.* (DESI), DESI 2024 IV: Baryon Acoustic Oscillations from the Lyman Alpha Forest, [arXiv:2404.03001 \[astro-ph.CO\]](#) (2024).
- [22] A. G. Adame *et al.* (DESI), DESI 2024 VI: Cosmological Constraints from the Measurements of Baryon Acoustic Oscillations, [arXiv:2404.03002 \[astro-ph.CO\]](#) (2024).
- [23] D. J. Eisenstein *et al.* (SDSS), Detection of the Baryon Acoustic Peak in the Large-Scale Correlation Function of SDSS Luminous Red Galaxies, *Astrophys. J.* **633**, 560 (2005), [arXiv:astro-ph/0501171](#).
- [24] S. Cole *et al.* (2dFGRS), The 2dF Galaxy Redshift Survey: Power-spectrum analysis of the final dataset and cosmological implications, *Mon. Not. Roy. Astron. Soc.* **362**, 505 (2005), [arXiv:astro-ph/0501174](#).
- [25] W. J. Percival, S. Cole, D. J. Eisenstein, R. C. Nichol, J. A. Peacock, A. C. Pope, and A. S. Szalay, Measuring the Baryon Acoustic Oscillation scale using the SDSS and 2dFGRS, *Mon. Not. Roy. Astron. Soc.* **381**, 1053 (2007), [arXiv:0705.3323 \[astro-ph\]](#).
- [26] W. J. Percival *et al.*, Baryon acoustic oscillations in the Sloan Digital Sky Survey Data Release 7 galaxy sample, *MNRAS* **401**, 2148 (2010), [arXiv:0907.1660 \[astro-ph.CO\]](#).
- [27] C. Blake *et al.*, The WiggleZ Dark Energy Survey: testing the cosmological model with baryon acoustic oscillations at  $z = 0.6$ , *MNRAS* **415**, 2892 (2011), [arXiv:1105.2862 \[astro-ph.CO\]](#).
- [28] C. Blake *et al.*, The WiggleZ Dark Energy Survey: mapping the distance-redshift relation with baryon acoustic oscillations, *MNRAS* **418**, 1707 (2011), [arXiv:1108.2635 \[astro-ph.CO\]](#).
- [29] E. A. Kazin *et al.*, The WiggleZ Dark Energy Survey: improved distance measurements to  $z = 1$  with reconstruction of the baryonic acoustic feature, *Mon. Not. Roy. Astron. Soc.* **441**, 3524 (2014), [arXiv:1401.0358 \[astro-ph.CO\]](#).
- [30] F. Beutler, C. Blake, M. Colless, D. H. Jones, L. Staveley-Smith, L. Campbell, Q. Parker, W. Saunders, and F. Watson, The 6dF Galaxy Survey: baryon acoustic oscillations and the local Hubble constant, *MNRAS* **416**, 3017 (2011), [arXiv:1106.3366 \[astro-ph.CO\]](#).
- [31] P. Carter, F. Beutler, W. J. Percival, C. Blake, J. Koda, and A. J. Ross, Low Redshift Baryon Acoustic Oscillation Measurement from the Reconstructed 6-degree Field Galaxy Survey, *Mon. Not. Roy. Astron. Soc.* **481**, 2371 (2018), [arXiv:1803.01746 \[astro-ph.CO\]](#).
- [32] L. Anderson *et al.*, The clustering of galaxies in the SDSS-III Baryon Oscillation Spectroscopic Survey: baryon acoustic oscillations in the Data Release 9 spectroscopic galaxy sample, *MNRAS* **427**, 3435 (2012), [arXiv:1203.6594 \[astro-ph.CO\]](#).
- [33] L. Anderson *et al.* (BOSS), The clustering of galaxies in the SDSS-III Baryon Oscillation Spectroscopic Survey: baryon acoustic oscillations in the Data Releases 10 and 11 Galaxy samples, *Mon. Not. Roy. Astron. Soc.* **441**, 24 (2014), [arXiv:1312.4877 \[astro-ph.CO\]](#).
- [34] S. Alam *et al.* (BOSS), The clustering of galaxies in the completed SDSS-III Baryon Oscillation Spectroscopic Survey: cosmological analysis of the DR12 galaxy sample, *Mon. Not. Roy. Astron. Soc.* **470**, 2617 (2017), [arXiv:1607.03155 \[astro-ph.CO\]](#).
- [35] M. Ata *et al.* (eBOSS), The clustering of the SDSS-IV extended Baryon Oscillation Spectroscopic Survey DR14 quasar sample: first measurement of baryon acoustic oscillations between redshift 0.8 and 2.2, *Mon. Not. Roy. Astron. Soc.* **473**, 4773 (2018), [arXiv:1705.06373 \[astro-ph.CO\]](#).
- [36] J. E. Bautista *et al.* (eBOSS), The Completed SDSS-IV extended Baryon Oscillation Spectroscopic Survey: measurement of the BAO and growth rate of structure of the luminous red galaxy sample from the anisotropic correlation function between redshifts 0.6 and 1, *Mon. Not. Roy. Astron. Soc.* **500**, 736 (2020), [arXiv:2007.08993 \[astro-ph.CO\]](#).
- [37] J. Hou *et al.* (eBOSS), The Completed SDSS-IV extended Baryon Oscillation Spectroscopic Survey: BAO and RSD measurements from anisotropic clustering analysis of the Quasar Sample in configuration space between redshift 0.8 and 2.2, *Mon. Not. Roy. Astron. Soc.* **500**, 1201 (2020), [arXiv:2007.08998 \[astro-ph.CO\]](#).
- [38] N. G. Busca *et al.*, Baryon acoustic oscillations in the Ly $\alpha$  forest of BOSS quasars, *A&A* **552**, A96 (2013), [arXiv:1211.2616 \[astro-ph.CO\]](#).
- [39] A. Font-Ribera *et al.* (BOSS), Quasar-Lyman  $\alpha$  Forest Cross-Correlation from BOSS DR11 : Baryon Acoustic Oscillations, *JCAP* **05**, 027, [arXiv:1311.1767 \[astro-ph.CO\]](#).
- [40] J. E. Bautista *et al.* (BOSS), Measurement of baryon acoustic oscillation correlations at  $z = 2.3$  with SDSS DR12 Ly $\alpha$ -Forests, *Astron. Astrophys.* **603**, A12 (2017), [arXiv:1702.00176 \[astro-ph.CO\]](#).
- [41] H. du Mas des Bourboux *et al.* (eBOSS), The Completed SDSS-IV Extended Baryon Oscillation Spectroscopic Survey: Baryon Acoustic Oscillations with Ly $\alpha$  Forests, *Astrophys. J.* **901**, 153 (2020), [arXiv:2007.08995 \[astro-ph.CO\]](#).
- [42] S. Alam *et al.* (eBOSS), Completed SDSS-IV extended Baryon Oscillation Spectroscopic Survey: Cosmological implications from two decades of spectroscopic surveys at the Apache Point Observatory, *Phys. Rev. D* **103**, 083533 (2021), [arXiv:2007.08991 \[astro-ph.CO\]](#).
- [43] E. V. Linder, Exploring the expansion history of the universe, *Phys. Rev. Lett.* **90**, 091301 (2003), [arXiv:astro-ph/0208512](#).
- [44] R. de Putter and E. V. Linder, Calibrating Dark Energy, *JCAP* **10**, 042, [arXiv:0808.0189 \[astro-ph\]](#).

- [45] N. Aghanim *et al.* (Planck), Planck 2018 results. VI. Cosmological parameters, *Astron. Astrophys.* **641**, A6 (2020), [Erratum: *Astron. Astrophys.* 652, C4 (2021)], [arXiv:1807.06209 \[astro-ph.CO\]](#).
- [46] N. Aghanim *et al.* (Planck), Planck 2018 results. V. CMB power spectra and likelihoods, *Astron. Astrophys.* **641**, A5 (2020), [arXiv:1907.12875 \[astro-ph.CO\]](#).
- [47] P. A. R. Ade *et al.* (Planck), Planck 2013 results. XVII. Gravitational lensing by large-scale structure, *Astron. Astrophys.* **571**, A17 (2014), [arXiv:1303.5077 \[astro-ph.CO\]](#).
- [48] P. A. R. Ade *et al.* (Planck), Planck 2015 results. XV. Gravitational lensing, *Astron. Astrophys.* **594**, A15 (2016), [arXiv:1502.01591 \[astro-ph.CO\]](#).
- [49] J. Carron, M. Mirmelstein, and A. Lewis, CMB lensing from Planck PR4 maps, *JCAP* **09**, 039, [arXiv:2206.07773 \[astro-ph.CO\]](#).
- [50] N. MacCrann *et al.* (ACT), The Atacama Cosmology Telescope: Mitigating the impact of extragalactic foregrounds for the DR6 CMB lensing analysis, [arXiv:2304.05196 \[astro-ph.CO\]](#) (2023).
- [51] F. J. Qu *et al.* (ACT), The Atacama Cosmology Telescope: A Measurement of the DR6 CMB Lensing Power Spectrum and Its Implications for Structure Growth, *Astrophys. J.* **962**, 112 (2024), [arXiv:2304.05202 \[astro-ph.CO\]](#).
- [52] M. S. Madhavacheril *et al.* (ACT), The Atacama Cosmology Telescope: DR6 Gravitational Lensing Map and Cosmological Parameters, *Astrophys. J.* **962**, 113 (2024), [arXiv:2304.05203 \[astro-ph.CO\]](#).
- [53] D. Brout *et al.*, The Pantheon+ Analysis: Cosmological Constraints, *Astrophys. J.* **938**, 110 (2022), [arXiv:2202.04077 \[astro-ph.CO\]](#).
- [54] D. Rubin *et al.*, Union Through UNITY: Cosmology with 2,000 SNe Using a Unified Bayesian Framework (2023), [arXiv:2311.12098 \[astro-ph.CO\]](#).
- [55] T. M. C. Abbott *et al.* (DES), The Dark Energy Survey: Cosmology Results With ~1500 New High-redshift Type Ia Supernovae Using The Full 5-year Dataset, [arXiv:2401.02929 \[astro-ph.CO\]](#) (2024).
- [56] A. Banerjee, H. Cai, L. Heisenberg, E. O. Colgáin, M. M. Sheikh-Jabbari, and T. Yang, Hubble sinks in the low-redshift swampland, *Phys. Rev. D* **103**, L081305 (2021), [arXiv:2006.00244 \[astro-ph.CO\]](#).
- [57] B.-H. Lee, W. Lee, E. O. Colgáin, M. M. Sheikh-Jabbari, and S. Thakur, Is local  $H_0$  at odds with dark energy EFT?, *JCAP* **04** (04), 004, [arXiv:2202.03906 \[astro-ph.CO\]](#).
- [58] E. O. Colgáin, M. G. Dainotti, S. Capozziello, S. Pourojaghi, M. M. Sheikh-Jabbari, and D. Stojkovic, Does DESI 2024 Confirm  $\Lambda$ CDM?, [arXiv:2404.08633 \[astro-ph.CO\]](#) (2024).
- [59] S. Tsujikawa, Quintessence: A Review, *Class. Quant. Grav.* **30**, 214003 (2013), [arXiv:1304.1961 \[gr-qc\]](#).
- [60] S. D. Storm and R. J. Scherrer, Swampland conjectures and slow-roll thawing quintessence, *Phys. Rev. D* **102**, 063519 (2020), [arXiv:2008.05465 \[hep-th\]](#).
- [61] N. Schöneberg, L. Vacher, J. D. F. Dias, M. M. C. D. Carvalho, and C. J. A. P. Martins, News from the Swampland — constraining string theory with astrophysics and cosmology, *JCAP* **10**, 039, [arXiv:2307.15060 \[astro-ph.CO\]](#).
- [62] M. Chevallier and D. Polarski, Accelerating universes with scaling dark matter, *Int. J. Mod. Phys. D* **10**, 213 (2001), [arXiv:gr-qc/0009008](#).
- [63] R. J. Scherrer, Mapping the Chevallier-Polarski-Linder parametrization onto Physical Dark Energy Models, *Phys. Rev. D* **92**, 043001 (2015), [arXiv:1505.05781 \[astro-ph.CO\]](#).
- [64] S. Dutta and R. J. Scherrer, Hilltop Quintessence, *Phys. Rev. D* **78**, 123525 (2008), [arXiv:0809.4441 \[astro-ph\]](#).
- [65] T. Chiba, Slow-Roll Thawing Quintessence, *Phys. Rev. D* **79**, 083517 (2009), [Erratum: *Phys. Rev. D* 80, 109902 (2009)], [arXiv:0902.4037 \[astro-ph.CO\]](#).
- [66] M. Cortês and A. R. Liddle, Interpreting DESI's evidence for evolving dark energy, [arXiv:2404.08056 \[astro-ph.CO\]](#) (2024).
- [67] A. G. Riess *et al.* (Supernova Search Team), Observational evidence from supernovae for an accelerating universe and a cosmological constant, *Astron. J.* **116**, 1009 (1998), [arXiv:astro-ph/9805201](#).
- [68] S. Perlmutter *et al.* (Supernova Cosmology Project), Measurements of  $\Omega$  and  $\Lambda$  from 42 High Redshift Supernovae, *Astrophys. J.* **517**, 565 (1999), [arXiv:astro-ph/9812133](#).
- [69] A. D. Linde, Fast roll inflation, *JHEP* **11**, 052, [arXiv:hep-th/0110195](#).
- [70] G. N. Felder, A. V. Frolov, L. Kofman, and A. D. Linde, Cosmology with negative potentials, *Phys. Rev. D* **66**, 023507 (2002), [arXiv:hep-th/0202017](#).
- [71] G. Obied, H. Ooguri, L. Spodyneiko, and C. Vafa, De Sitter Space and the Swampland, [arXiv:1806.08362 \[hep-th\]](#) (2018).
- [72] S. K. Garg and C. Krishnan, Bounds on Slow Roll and the de Sitter Swampland, *JHEP* **11**, 075, [arXiv:1807.05193 \[hep-th\]](#).
- [73] H. Ooguri, E. Palti, G. Shiu, and C. Vafa, Distance and de Sitter Conjectures on the Swampland, *Phys. Lett. B* **788**, 180 (2019), [arXiv:1810.05506 \[hep-th\]](#).
- [74] G. Dvali and C. Gomez, On Exclusion of Positive Cosmological Constant, *Fortsch. Phys.* **67**, 1800092 (2019), [arXiv:1806.10877 \[hep-th\]](#).
- [75] G. Dvali, C. Gomez, and S. Zell, Quantum Breaking Bound on de Sitter and Swampland, *Fortsch. Phys.* **67**, 1800094 (2019), [arXiv:1810.11002 \[hep-th\]](#).
- [76] D. Andriot, On the de Sitter swampland criterion, *Phys. Lett. B* **785**, 570 (2018), [arXiv:1806.10999 \[hep-th\]](#).
- [77] D. Andriot and C. Roupec, Further refining the de Sitter swampland conjecture, *Fortsch. Phys.* **67**, 1800105 (2019), [arXiv:1811.08889 \[hep-th\]](#).
- [78] P. Agrawal, G. Obied, P. J. Steinhardt, and C. Vafa, On the Cosmological Implications of the String Swampland, *Phys. Lett. B* **784**, 271 (2018), [arXiv:1806.09718 \[hep-th\]](#).
- [79] A. Achúcarro and G. A. Palma, The string swampland constraints require multi-field inflation, *JCAP* **02**, 041, [arXiv:1807.04390 \[hep-th\]](#).
- [80] W. H. Kinney, S. Vagnozzi, and L. Visinelli, The zoo plot meets the swampland: mutual (in)consistency of single-field inflation, string conjectures, and cosmological data, *Class. Quant. Grav.* **36**, 117001 (2019), [arXiv:1808.06424 \[astro-ph.CO\]](#).
- [81] S. Brahma and M. Wali Hossain, Avoiding the string swampland in single-field inflation: Excited initial states, *JHEP* **03**, 006, [arXiv:1809.01277 \[hep-th\]](#).
- [82] S. Das, Note on single-field inflation and the swampland criteria, *Phys. Rev. D* **99**, 083510 (2019), [arXiv:1809.03962 \[hep-th\]](#).
- [83] H. Fukuda, R. Saito, S. Shirai, and M. Yamazaki, Phenomenological Consequences of the Refined Swampland Conjecture, *Phys. Rev. D* **99**, 083520 (2019), [arXiv:1810.06532 \[hep-th\]](#).
- [84] A. Ashoorioon, Rescuing Single Field Inflation from the Swampland, *Phys. Lett. B* **790**, 568 (2019),

- [arXiv:1810.04001 \[hep-th\]](#).
- [85] Y. Nakai, R. Namba, I. Obata, Y.-C. Qiu, and R. Saito, Can we explain cosmic birefringence without a new light field beyond Standard Model?, *JHEP* **01**, 057, [arXiv:2310.09152 \[astro-ph.CO\]](#).
  - [86] D. Klaewer and E. Palti, Super-Planckian Spatial Field Variations and Quantum Gravity, *JHEP* **01**, 088, [arXiv:1610.00010 \[hep-th\]](#).
  - [87] F. Baume and E. Palti, Backreacted Axion Field Ranges in String Theory, *JHEP* **08**, 043, [arXiv:1602.06517 \[hep-th\]](#).
  - [88] M. Scalisi and I. Valenzuela, Swampland distance conjecture, inflation and  $\alpha$ -attractors, *JHEP* **08**, 160, [arXiv:1812.07558 \[hep-th\]](#).
  - [89] N. Arkani-Hamed, L. Motl, A. Nicolis, and C. Vafa, The String landscape, black holes and gravity as the weakest force, *JHEP* **06**, 060, [arXiv:hep-th/0601001](#).